3D FE seismic analysis of a monopile-supported offshore wind turbine in a non-liquefiable soil deposit

Vacareanu, Vlad; Kementzetzidis, Vagelis; Pisano, Federico

Publication date
2019

Document Version
Final published version

Published in
Proceedings of the 2nd International Conference on Natural Hazards & Infrastructure

Citation (APA)
Vacareanu, V., Kementzetzidis, V., & Pisano, F. (2019). 3D FE seismic analysis of a monopile-supported offshore wind turbine in a non-liquefiable soil deposit. In G. Gazetas, & I. Anastasopoulos (Eds.), *Proceedings of the 2nd International Conference on Natural Hazards & Infrastructure* (Proceedings of the International Conference on Natural Hazards and Infrastructure). National Technical University of Athens.

ICONHIC2019
2nd International Conference on Natural Hazards & Infrastructure
23-26 June, 2019, Chania, Greece

3D FE seismic analysis of a monopile-supported offshore wind turbine in a non-liquefiable soil deposit

V. Vacareanu, E.Kementzetzidis, F. Pisanò[1],
Delft University of Technology

ABSTRACT

Japan is one of the most seismically active countries in the world, and is currently planning to invest on offshore wind energy. In support of this relevant energy transition, this work presents a numerical study regarding a monopile-supported offshore wind turbine (OWT) under seismic loading conditions. For this purpose, a realistic design of an 8 MW OWT is considered, wished-in-place in a layered, non-liquefiable Japanese site. The OWT seismic response is analysed via 3D FE modelling incorporating for the soil the well-established SANISAND bounding surface plasticity model, and thus enabling realistic simulation of the cyclic hydro-mechanical response of the coarse-grained materials at the considered site. Site data regarding soil stratigraphy and past earthquake records were obtained from the well-known Japanese KiK-net database. From these data, the 15 parameters of the SANISAND model were calibrated by combining back-analysis of seismic records and available linear elastic soil properties.
The influence of different intensity earthquake records on the response of the OTW-monopile-soil system is examined both for horizontal and vertical seismic components. Even in a non-liquefiable site, pore pressure effects and their impact on the structural response are clearly visible in the simulation results. The likely coexistence of seismic and SLS wind/wave loading is also considered for completeness.

Keywords: earthquakes, offshore wind turbines, soil plasticity, 3D FE modelling,

INTRODUCTION

A few decades ago, the concept of environmental sustainability was unknown to most people, whereas commitment to reducing carbon footprint is becoming nowadays a distinctive feature of developed societies. Relatedly, harvesting energy from offshore wind has become a booming industry. To date, Europe is the main offshore wind market, with America and Asia expected to increase their share in the very near future (Ushiyama, 2018). This study devotes special attention to the green energy transition taking place in Japan.
Prior to the Fukushima nuclear disaster[2], the energy plan of the Japanese government was to increase the nuclear share in the electricity mix to about 50% by 2030[3]. After Fukushima, Japanese decision-makers set plans to diversify energy sources in the country. Such a goal is not easy to achieve as Japan has remarkable energy demands due to its vast manufacturing industry. To ensure sufficient energy inflow into the power grid, the Japanese Ministry of Environment has assessed the local potential of both onshore and offshore wind power. According to (Arakawa & Ueda, 2012) 280GW and 1600GW of energy can be harvested from the exploitation of onshore and offshore wind. The Japan Wind Power Association has drawn a road map regarding the expected utilisation of wind power in the foreseeable future. A considerable amount of the

[1] Corresponding Author: *Federico Pisanò, Delft University of Technology, F.Pisano@tudelft.nl*
[2] Nuclear meltdown on 11th March 2011, caused by an earthquake-induced tsunami *(https://en.wikipedia.org).*
[3] The Japan Times, 2013, *https://www.japantimes.co.jp*

electricity input will stem from offshore wind by 2050, with fixed-based offshore wind turbines taking the largest share of offshore-generated energy (19GW).

Natural Hazards

Japan is one of the most seismically active countries in the world. Located in the ring of fire, the country is located at the junction of the North American, Pacific, Eurasian and Philippine tectonic plates. About 90% of the world's earthquakes and 81% of the world's largest ones occur in this region[4]. With reference to the harvesting of offshore wind energy, one of the main challenges for Japan's ambitions is embodied by the seismicity of the region and the serious engineering difficulties it brings about. Large-diameter monopile foundations have largely been employed so far in non-seismic areas (i.e. in the North Sea), but there is very limited experience about their response during earthquake events. The findings of this study are also relevant to the Taiwanese offshore industry, currently facing similar seismicity issues (Zhang, et al., 2017).

Structural analysis and soil-structure interaction

OWT turbines are long-period structures often considered to be earthquake-immune (Witcher, 2005; Bazeos, et al., 2002). Nevertheless, as recently demonstrated for OWT on suction caissons, while earthquake-induced ULS (ultimate limit state) failure is unlikely, accumulated deflections in SLS (serviceability limit state) can become hazardous (Kourkoulis, et al., 2014). Another issue that must be examined in OWT structures is the effect of seismic vertical motion, generally neglected by structural engineers in light of the high safety factors applied to gravity loads. Tall/slender structures as OWTs are considered to be vulnerable with respect to combined vertical and horizontal vibrations (Pitilakis, 2010). Since OWTs house acceleration-sensitive equipment, it is also of interest to examine how seismically-induced vertical accelerations are transmitted to the nacelle, i.e. where fine-tuned equipment is located (Kjorlaug, 2013).

A few studies have been carried out on the seismic performance of OWTs – see the recent review by (Katsanos, et al., 2016). It was concluded that the modelling of seismically loaded OWTs can more favourably be tackled (Kaynia, 2018) through fully integrated FE models, including proper description of both the wind turbine structure and the soil-foundation system. An example of seismic analysis of OWTs on caisson or tripod foundations is provided by (Kaynia, 2018) in combination with the use of macro-foundation models. The study concluded that earthquake events can have detrimental effects on the long-term OWT response, owing to foundation settlement and permanent tilting. The same study warned about soil non-linearity and pore water pressures possibly affecting the seismic response of the structure. An analytical procedure was presented to evaluate the seismic assessment of monopile-supported offshore wind turbines (Risi, et al., 2018) in presence of different types of earthquake – crustal, in slab and interface. The study concluded that during earthquakes the effect of higher structural modes cannot be neglected. Additionally, it was reported that inadequate SSI modelling can lead to an overestimation of the seismic resistance of about 60% and 70% for the SLS and ULS, respectively. Local buckling and related limit state are also a relevant concern in presence of moderate to strong seismic motion.

Case study

This work presents an example of integrated OWT analysis in presence of (Japanese) seismic loading. An 8-MW Siemens Gamesa OWT[5] is modelled at a "semi-fictional" offshore site in Japan – real offshore site data were not available. A coastal site was chosen to approximate offshore conditions: this was considered an acceptable choice, as the deep waters achieved not far from the Japanese coastline would already pose a limit to the use of large-diameter monopiles at near-shore locations. The site – see stratigraphy in Table 1 – was selected from the well-known strong-motion seismic network KiK-net[6]. Among the available stations, attention was devoted to the FKSH14 station, located on a mainly sandy, hardly liquefiable site in central Japan (Roten, et al., 2014). Earthquake records from FKSH14 were extracted based on their acceleration magnitude, including an accelerogram from the infamous Tohoku earthquake (2011) and another 225 gal record – henceforth referred to as 225 gal (see Figure 1). The purpose was to explore the influence of varying seismic magnitude on the OWTs dynamic response. For these records the OWT structural performance was analysed in relation to buckling issues and transmission of vertical accelerations to hub-nacelle equipment.

[4] *https://www.usgs.gov*

[5] Foundation designed for a medium dense to dense sand deposit in the North Sea.

[6] Kik-net is part of NIED, the National Research Institute for Earth Science and Disaster Resilience.

Table 1. FKSH14 site stratigraphy

Type	Sand	Gravel	Silt	Bedrock
Depth(m)	0-20	20-60	60-85	85-150

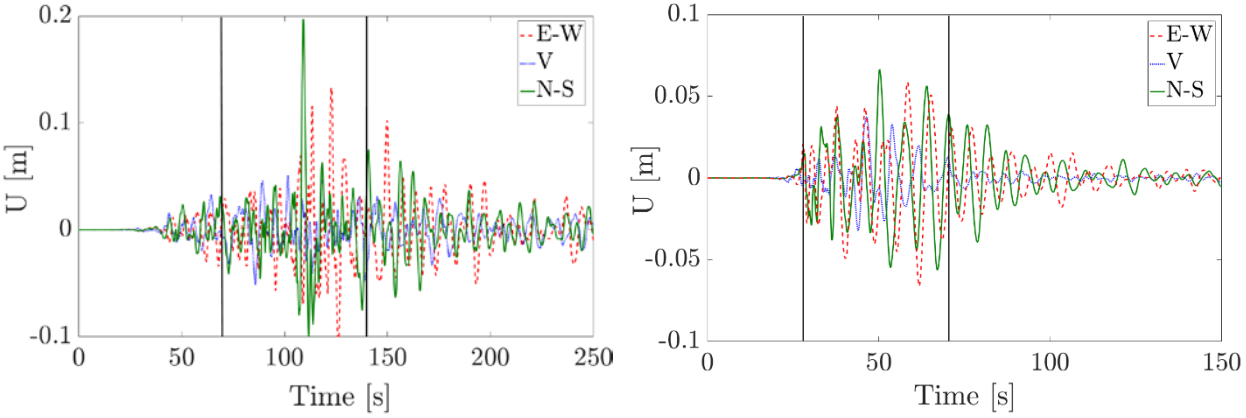

Figure 1. Borehole displacement measurements from FKHS14 station for Tohoku (left) and 225 gal (right) earthquake. In each figure the East West (E-W), the vertical (V) and the North-South (N-S) recorded components are displayed. Black vertical lines denote significant signal duration based on Arias intensity.

3D FE MODELLING

A 3D FE model of the whole soil-monopile-OWT system was built through the OpenSees simulation platform (http://opensees.berkeley.edu; (McKenna 1997)). Modelling ingredients and description of the considered OWT are available in (Kementzetzidis, et al., 2019a) and only summarised hereafter. To calibrate appropriate soil parameters, a 1D column model was created and used to identify soil properties by matching recorded and calculated soil motion at the FKSH14 station – bedrock and surface motions considered.

Soil domain and cyclic sand modelling

The dynamics of the water-saturated soil at relatively low frequencies was described via the u–p formulation by Zienkiewicz and coworkers, based on the assumption of negligible soil-fluid relative acceleration (Zienkiewicz, et al., 1999). Spurious checkerboard pore pressure modes near the 'undrained-incompressible limit' were avoided by employing the H1-P1ssp stabilised elements proposed by (McGann, et al., 2015). These 8-node equal order brick elements exploit a non-residual-based stabilisation controlled by a numerical parameter α calibrated as a function of the average element size and elastic moduli of the soil skeleton.
This study relies on the predictive capability of the SANISAND04 model by (Dafalias & Manzari, 2004), available in OpenSees after the implementation developed at the University of Washington (Ghofrani & Arduino, 2018)**.** The SANISAND04 model stands out for capturing the cyclic response of sands on symmetric cyclic loading, across a range of effective confinement stresses and relative densities. The aforementioned is achieved with a single set of 15 parameters.

OWT and monopile structures

The OWT-monopile set-up assumed in this study is representative of the current industry practice and concerns a large 8 MW OWT. Relevant structural details – courtesy of Siemens Gamesa Renewable Energy – have been all incorporated in the numerical model, although not completely reported herein to protect confidential information. An overview is provided in Figure 2, with more details available in (Kementzetzidis, et al., 2018). The steel structure above the mudline (wind tower and part of the monopile) was modelled as an elastic beam with variable cross-section, and subdivided into Timoshenko beam elements with consistent mass matrix. The embedded portion of the tubular monopile was instead modelled as a 3D hollow cylinder, discretised by using 8-node, one-phase ssp bricks (H1ssp). The OWT mode also includes structural and equipment masses (flanges, transition piece, boat landing and working platforms, etc.), as well as the RNA lumped mass MRNA (Rotor-Nacelle Assembly) at the top with rotational inertia

IM associated with nacelle mass imbalances. Added mass effects due to the surrounding sea water were simplistically introduced as nodal lumped masses evenly distributed along the water depth H_w=30m and calculated as twice the water mass in the submerged OWT volume (Newman, 1977). The sharp HM (Hydro-Mechanical) discontinuity at the sand-pile interface was handled by inserting a thin continuum layer of 'degraded' material around the monopile, both along its shaft and under the tip. The weaker interface sand features elastic shear modulus and critical stress ratio 2/3 and 3/4 times lower than in the intact material of each layer of soil in contact with the pile, respectively. In this study, the simulation of pile installation has not been attempted for the sake of simplicity – readers are referred, for instance, to (Galavi, et al., 2017; Anusic, et al., 2017; Tehrani, et al., 2016) for studies concerning the modelling and implications of installation effects in piled foundations.

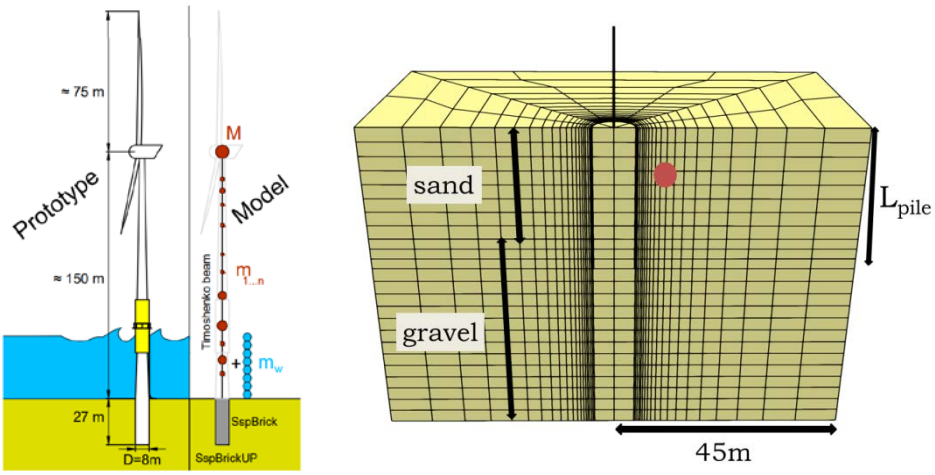

Figure 2. (left) Idealisation and FE modelling of the OWT-foundation-soil system, (right) 3D soil mesh with position of control points.

Energy dissipation

A major issue in the dynamic simulation of OWTs concerns the modelling of all sources of energy dissipation (damping). In particular, most energy dissipation takes place within the soil domain as plastic/hysteretic damping and wave radiation away from the monopile. In this study the lateral boundary degrees of freedom were tied (TDOF) according to (Zienkiewicz, et al., 1989) and absorbing viscous dampers were added to allow for wave radiation where deemed appropriate, although with issues similar to those reported by (Kontoe, et al., 2007). According to these authors, applying only the TDOF boundary conditions has been reported to perform satisfactory when radiating waves towards the boundaries are sufficiently damped – in their study through soil plasticity and a reasonably large domain. Structural damping was introduced at all the steel sections based on (Eurocode 1, 2005). Rayleigh damping ratio ζ_{steel} = 0.19% was assigned to all steel cross sections at the pivot frequencies 0.1 and 80 Hz. Hydrodynamic damping was incorporated following (Leblanc & Tarp-Johansen, 2010), where a damping ratio of 0.12% due to wave radiation was obtained for an OWT with first natural bending frequency f_0 = 0.3 Hz, pile diameter of 4.7 m and water depth at 20 m. Due to lack of more specific data, a damping ratio of ζ_w = 0.12% was assigned to the added water mass nodes (Figure 2); aerodynamic damping was not included.

Space and time discretisation

To reduce the computational burden only half of the whole domain was modelled. This allowed to simulate, besides the vertical seismic component, only one of the two recorded horizontal earthquake components – the N-S component for both earthquakes was chosen (Figure 1). In earthquake engineering applications, a general rule of thumb for accurate capturing of propagating waves, is to discretise the spatial domain with 8 to 10 elements per wavelength. Accordingly, the shortest wavelength becomes critical, estimated through $\lambda = V_{s,min}/f_{max}$, with $V_{s,min}$ the lowest shear wave velocity and f_{max} the highest examined frequency. After inspecting the frequency spectrum of the input signals, it was decided that the highest resolved frequency would be 10 Hz – which yields an average element size of 2.63 meters. Time marching was performed through the Newmark algorithm with integration parameters β = 0.6 and γ = 0.3025, combined with explicit

forward Euler integration of soil constitutive equations at each stress point. A time-step size of 0.005 sec was set based on (Watanabe, et al., 2017), and sensitivity studies not reported for brevity.

Identification of soil parameters

A back-analysis approach was followed to identify SANISAND04 soil parameters for the site considered. A 150 m 1D soil column was modelled in OpenSees allowing for 3-directional seismic motion at the rigid bedrock (imposed displacement time histories). Soil parameters were calibrated by trial-and-error, with a stratigraphy compatible with borehole data. The silt and the sandstone layers were modelled as one-phase elastic-isotropic materials, with parameters suggested from (Roten, et al., 2014). The SANISAND04 material was used to simulate the upper 60 meters of the borehole (gravel and sand). Inferring 15 constitutive parameters through mere back-analysis would be apparently challenging, so it was preferred to adopt as a template the SANISAND04 parameter set provided by (Zahmatkesh & Janalizadeh Choobbasti, 2017) for the non-liquefiable Babolsar sand.

The adopted SANISAND04 parameters are listed in Table 2, while the comparison between measured and calculated surface motion can be seen in Figure 4 for the Tohoku N-S displacement component. Both earthquake signals and all their seismic components were cross-validated in both time and frequency domains. In all cases the response was adequately captured – the full set of results is omitted herein for brevity. To further reduce the time for computations, the lower rocky and silty layers were excluded from the OWT-monopile-soil column analysis. It was verified that these layers are stiff enough to rigidly transmit the seismic motion without appreciable amplification effects.

Table 2. SANISAND04 constitutive parameters and domain hydraulic conductivity

	Elasticity		Critical State					Plastic modulus		
Type	G_0	ν	M	c	λ_c	e_0	ξ	h_0	c_h	n^b
Sand	180	0.3	1.65	0.682	0.018	0.781	0.7	50.99	1.248	1.51
Gravel	220	0.3	1.9	0.682	0.018	0.781	0.7	50.99	1.248	1.51

	Dilatancy		Fabric		Permeability
Type	A_0	n^d	z_{max}	c_z	k(m/s)
Sand	0.008	7.51	35	700	3.0E-4
Gravel	0.008	7.51	35	700	1.0E-2

FE analysis of OWT-monopile-soil system

The passage from 1D column analysis to full 3D OWT-monopile-soil simulations required the specification of the lateral domain size. After careful sensitivity analysis, it was concluded that an acceptable trade-off between computational burden and accuracy is achieved by adopting a lateral domain of 90 meters in size (Figure 2). The full model was built and shaken at the lower boundary by applying the significant duration (Arias intensity) of the recorded (FKSH14) displacement time histories for both the Tohoku and the 225 gal earthquakes – Vertical and N-S components.

SLS environmental loads

For completeness of the study, wind and wave loads were considered as well. (Kiyomia, et al., 2002) concluded that in combination with earthquake loads, SLS wind and waves should be used (adopted in this study), as the probability of an earthquake occurring at the same time as ULS wind and waves is extremely small. To generate these loads, the procedure presented in (Corciulo, et al., 2017) was used. The procedure describes how to obtain from wind velocity time histories the wind and wave load time histories. The Pierson-Moskowitz wave spectrum (Pierson, et al., 1964) was assumed to estimate the wave energy associated with each loading frequency. In order to generate those load time histories, the software FAST[7] was used. (Tsuchiya, et al., 2006) calculated the mean wind speed and the turbulence intensity in offshore North-East Japan. The wind load has been applied as a point load at the hub, while the wave load has been applied as a point load at the mean sea level. Both load time histories can be seen in Figure 3.

[7] *https://nwtc.nrel.gov/FAST*

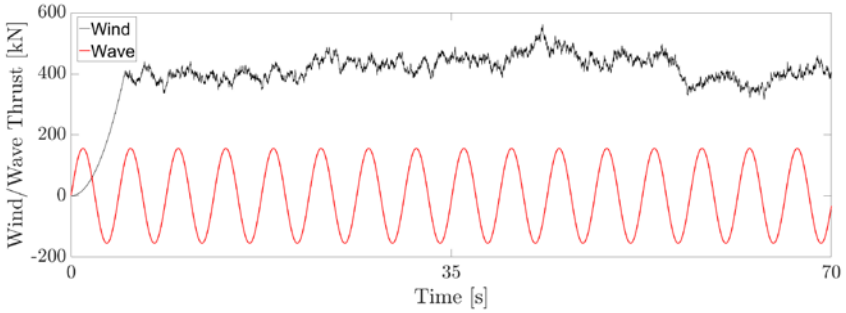

Figure 3. Wind and wave thrust forces for SLS environmental loading.

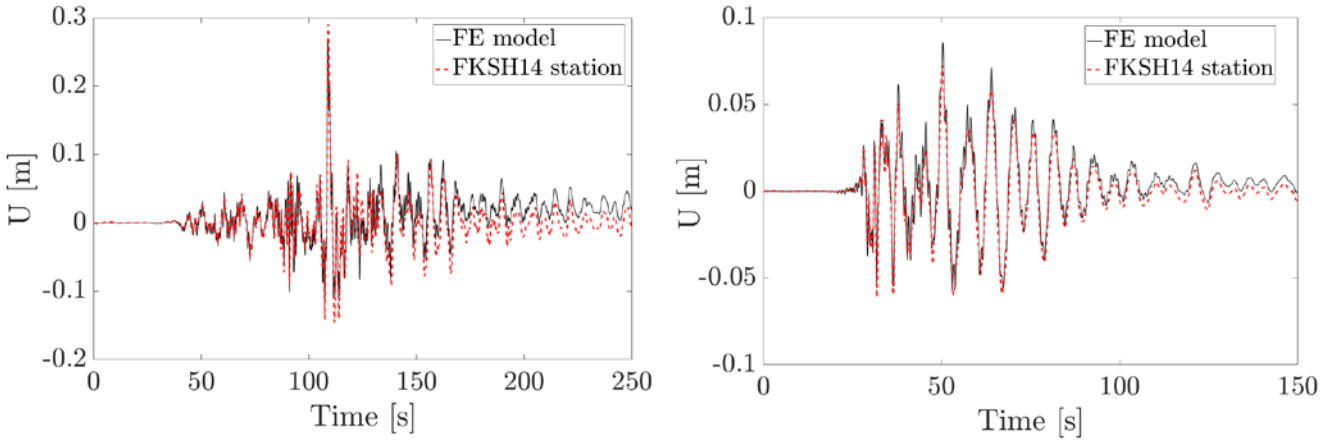

Figure 4. Comparison between calculated and measured displacement (U) at the soil surface for Tohoku (left) and 225 gal (right) seismic excitations (N-S horizontal component).

RESULTS

The simulated response of the soil deposit was mainly inspected in terms of pore pressure build-up and stress-strain cycles. The u/p ratio (between pore pressure and total mean stress) and shear stress versus shear strain on the x-z plain are illustrated in Figure 5 for the control point highlighted in red in Figure 2. Strong non-linear hydro-mechanical effects are most evident in the case with strongest/most violent shaking (Tohoku), which indicates significant alteration/damage of the foundation soil. Comparing soil straining and u/p ratios, the SLS environmental load case turns out to be practically insignificant against the effects of earthquake motion. It is worth noting that both u/p and τ_{xz}-γ_{xz} plot highlight that dilative soils display under strong shearing an increase in capacity, due to dilatancy-driven negative excess pore pressure. For the hardly liquefiable site under consideration, no seismic liquefaction was in fact simulated, except for the initial analysis stage associated with P-wave arrivals. Nonetheless, the initial pore pressure spikes had no impact on the subsequent OWT response, since liquefaction-induced damage takes time to develop (Kramer, et al., 2016). It was also possible to observe the OWT influence zone in the soil domain, that is the distance from the monopile beyond which free-field conditions may be assumed. As expected, such influence zone depends on the earthquake magnitude, and extends to approximately 3.5-4 D (monopile diameters) for the Tohoku and 1.5 D for the 225 gal shaking – and 0.5 D for the case with only SLS environmental loading. Although not reported for brevity, both foundation rotation and lateral displacement were found to be significantly larger under severe earthquake events than under SLS wind/wave loading a fact that is in agreement with observations by (Kaynia, 2018).

OWT dynamic response

The seismic response of the OWT is examined by means of time-frequency analysis based on Stockwell transformation (Stockwell, et al., 1996), a tool already proven useful to inspect the dynamics of OWTs (Kementzetzidis, et al., 2018; Kementzetzidis, et al., 2019a). Only results regarding the Tohoku earthquake (input signal S-transform for the N-S direction and OWT response seen on Figure 6) are presented in the following, with emphasis on the frequency content of the lateral OWT response. The hub-displacement response seems to be dominated by the first bending mode during the Tohoku excitation ($f/f_{FB}\approx1$). As the

OWT can be approximately regarded as a cantilever with a considerable mass at the top, then it is expected that a load input at the hub near the OWTs first cantilever eigenfrequency will be significantly amplified. It is interesting to note that after 40 seconds of earthquake shaking, the dominant frequency in the structural response seems to increase, in a way hardly attributable to the input. This could indicate, that strong motions in non-liquefiable, fully-saturated sandy soils can induce transient foundation stiffening, and in turn a shift in the structural eigenfrequencies. In further support of such statement, Figure 5 shows that after 40 seconds of shaking, the u/p ratio is on average lower than under hydrostatic conditions (t=0), which implies higher stiffness and shear resistance of the soil.

The geotechnical design of the monopile should be performed according to the response expected at the foundation itself. Therefore, the frequency content of the monopile head response is plotted in Figure 6. It is interesting to note the differences in dynamic response at the hub and at the monopile head. The monopile oscillates significantly at higher frequencies compared to the eigenfrequency of the first mode ($f/f_{FB}\approx1$), on what is considered to be the second structural mode ($f/f_{FB}\approx4$), within a frequency range where dynamic soil-foundation interaction effects cannot be neglected. Dynamic foundation effects for large diameter monopiles have been scarcely addressed so far (Kementzetzidis, et al., 2019b; Shadlou & Bhattacharya, 2016).

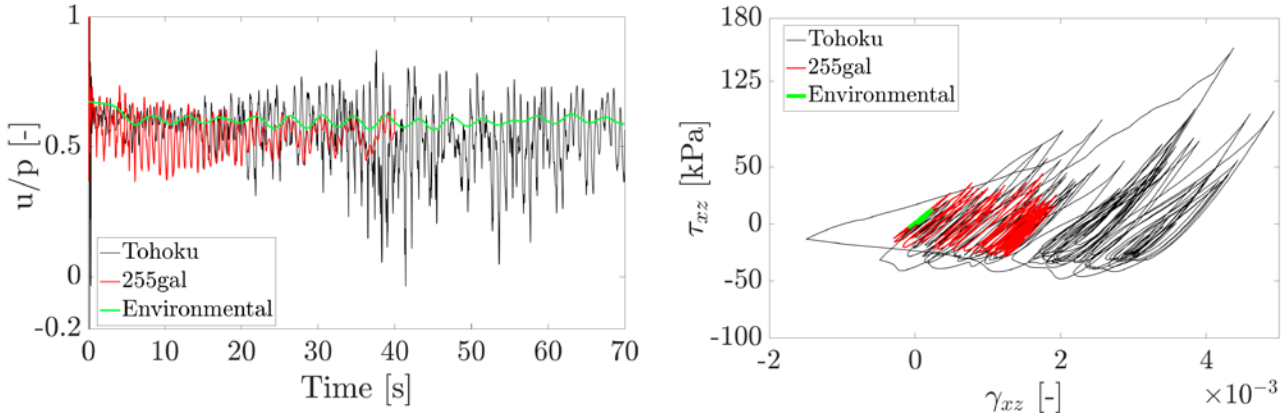

Figure 5. u/p ratio against time (left) and shear stress vs shear strain (right) for the examined control point. u/p=1 corresponds to full liquefaction.

Acceleration sensitive equipment

According to (Dueñas-Osorio & Basu, 2008) there is evidence that the functionality of industrial equipment can be jeopardised by moderate to high vertical accelerations. For instance, the functionality of generators, inverters and electrical can be negatively affected by acceleration amplitudes of 5-10 m/s^2, 10-15 m/s^2 and 15-20 m/s^2, respectively. In Figure 7 the vertical acceleration at the hub calculated for the Tohoku seismic event is shown. It is obvious that the 5 m/s^2 acceleration threshold is exceeded, so that equipment damage under seismic loading seems to be possible.

Buckling analysis

As OWTs are slender steel structures subjected to large axial forces during lateral vibration, buckling checks are inevitably very relevant to structural design. When designing an OWT to be operating at a seismic site, the additional bending and axial loads induced by foreseen seismic events shall be considered. Accordingly, the procedure described in (Eurocode 3, 2007) was followed to assess the OWT design against both meridional and shear buckling. For this purpose, the maximum buckling stress along the structure was obtained by examining the evolution in time of pairs of moment, axial and shear force. Following the procedure recommended for long shells, the safety factor (capacity over demand) against meridional buckling stress is plotted Figure 7 (the structure was found safe against shear bucking). It is concluded that the considered structural design (not meant for seismic loading) cannot withstand buckling under strong seismic events.

CONCLUSIONS

In this study 3D FE analysis were carried to shed light on the seismic response of OWTs in combination with site conditions likely to be found offshore Japan. Two earthquake records and SLS wind/wave load cases were compared highlighting the severity of strong seismic events on long-period slender structures. Even in a non-liquefiable soil, strong soil non-linearity is mobilised which may jeopardize the integrity and durability of the structure. An interesting interplay between soil capacity and seismic severity is observed while it is shown that eigenfrequency shifts are possible as soil stiffness changes due to its hydro-mechanical response. Stockwell-transforms of the monopile head displacement showed that during seismic events the monopile response could peak at frequencies higher than for the OWT hub, with the occurrence of substantial dynamic amplification effects at the foundation level.
Earthquake induced accelerations can potentially compromise the functionality of equipment located at the hub, while buckling stress checks highlighted that different provisions need to be accounted for in presence of seismic loading.

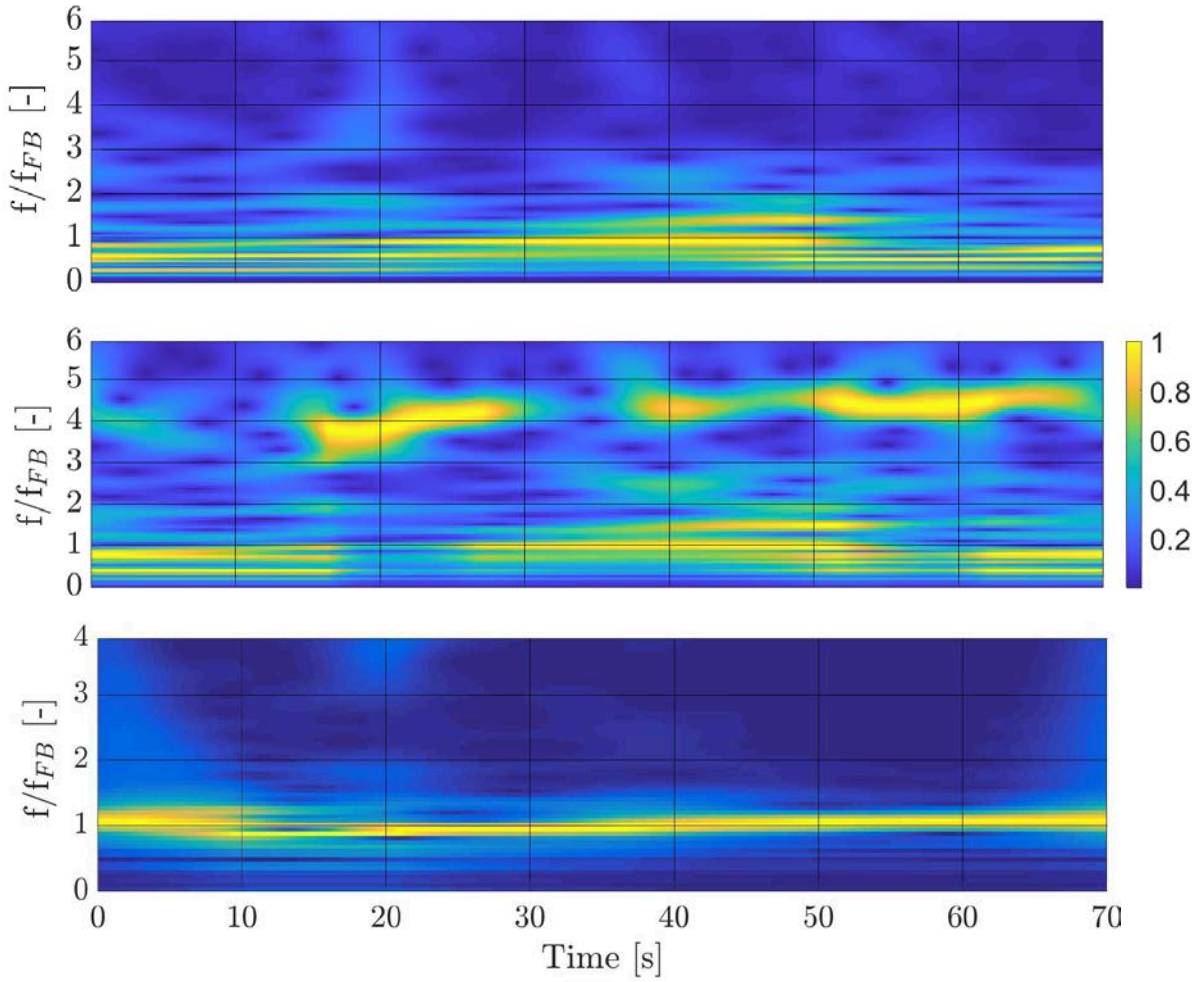

Figure 6. S-plots of (top) seismic input at the bedrock for the N-S direction, pile head lateral displacement (middle) and hub lateral displacement (bottom) against time. Colorbar indicates amplitude of all harmonics.

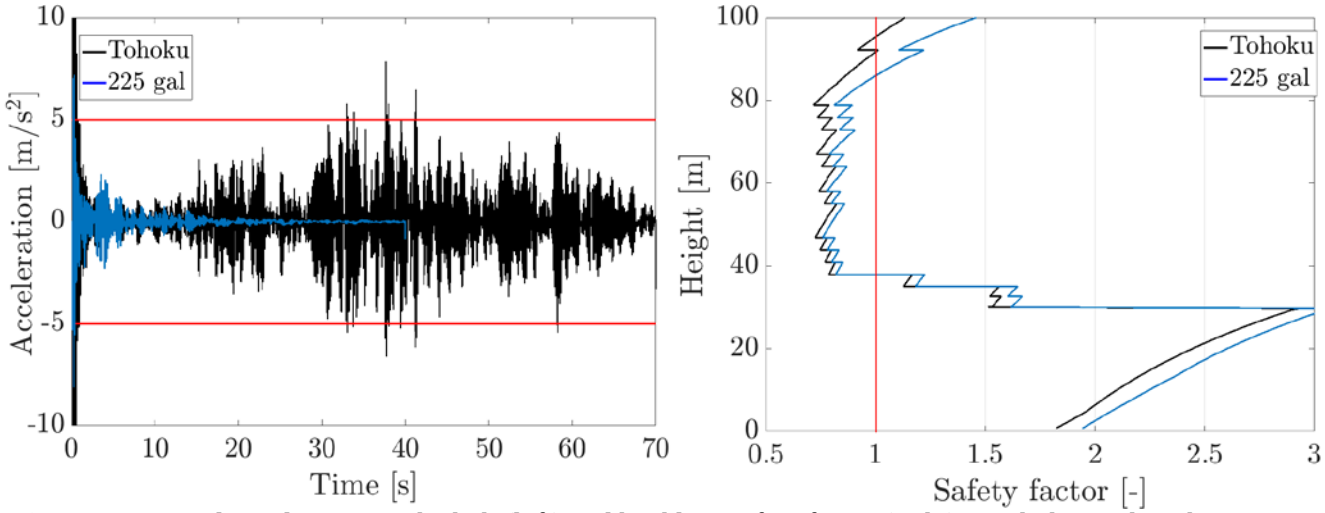

Figure 7. Vertical acceleration at the hub (left) and buckling safety factor (right) – Tohoku earthquake case.

REFERENCES

Anusic, I., Eiksund, G. R., Meissl, S. & Liingaard, M. A., 2017. *Study of a new installation technique for large diameter monopiles.* s.l., Proceedings of the 19th International Conference on Soil Mechanics and Geotechnical Engineering.

Arakawa, C. & Ueda, Y., 2012. *Development of wind power in Japan after disaster of earthquake and,* Copenhagen: European Wind Energy Association.

Atkinson G.M. , D. Wald, C.B. Worden, V. Quitoriano, 2018. The Intensity Signature of Induced Seismicity. *Bulletin of the Seismological Society of America*, 108(3a), pp. pp. 1080-1086.

Bazeos, N. et al., 2002. Static, seismic and stability analyses of a prototype wind turbine steel tower. *Engineering Structures,* pp. 1015 - 1025.

Corciulo, S., Zanoli, O. & Pisanò, F., 2017. Transient response of offshore wind turbines on monopiles in sand: role of cyclic hydro--mechanical soil behaviour. *Computers and Geotechnics,* Volume 83, pp. 221-238.

Corti, R. et al., 2016. Memory surface hardening model for granular soils under repeated loading conditions. *Journal of Engineering Mechanics.*

Dafalias, Y. F. & Manzari, M. T., 2004. Simple plasticity sand model accounting for fabric change effects. *Journal of Engineering mechanic,* Volume 130, pp. 622-634.

Dueñas-Osorio, L. & Basu, B., 2008. Unavailability of wind turbines due to wind-induced accelerations. *Engineering Structures,* pp. 885 - 893.

Eurocode 1, 1., 2005. *EN 1991-1-4, Eurocode 1: Actions on structures - Part 1-4: General actions - Wind actions,* s.l.: s.n.

Eurocode 3, 3., 2007. *EN 1993-1-6, Eurocode 3: Design of steel structures - Part 1-6: Strength and Stability of Shell Structures,* s.l.: s.n.

Galavi, V. et al., 2017. *Numerical simulation of pile installation in saturated sand using material point method.* s.l., Procedia Engineering 175.

Ghofrani, A. & Arduino, P., 2018. Prediction of LEAP centrifuge test results using a pressure-dependent bounding surface constitutive model. *Soil Dynamics and Earthquake Engineering,* Volume 113, pp. 758-770.

Huang, M., Yue, Z. Q., Tham, L. G. & Zienkiewicz, O. C., 2004. On the stable finite element procedures for dynamic problems of saturated porous media. *International Journal for Numerical Methods in Engineering,* Volume 61, pp. 1421-1450.

Hughes, T. J. R., 1987. *The Finite Element Method: linear static and dynamic finite element analysis.* s.l.:Prentice-Hall.

Katsanos, E. I., Thöns, S. & Georgakis, C. T., 2016. Wind turbines and seismic hazard: a state-of-the-art review. *Wind Energy,* Volume 19, pp. 2113-2133.

Kaynia, A. M., 2018. Seismic considerations in design of offshore wind turbines. *Soil Dynamics and Earthquake Engineering.*

Kementzetzidis, E., Corciulo, S., Versteijlen, W. & Pisanò, F., 2019a. Geotechnical aspects of offshore wind turbine dynamics from 3D non-linear soil-structure simulations. *Soil Dynamics & Earthquacke Engineering.*

Kementzetzidis, E., Metrikine, A., Versteijlen, W. & Pisanò, F., 2019b. Dynamic stiffness of monopiles supporting offshore wind turbine generators and Frequency effects in the dynamic lateral stiffness of monopiles in sand (sent for publication). *Géotechnique.*

Kementzetzidis, E., Versteijlen, W. G., Nernheim, A. & Pisanò, F., 2018. 3D FE dynamic modelling of offshore wind turbines in sand: natural frequency evolution in the pre– to after-storm transition.

Kiyomia, O., Rikiji, T., Gelder, V. & Pieter, H. A. J. M., 2002. *Dynamic Response Analysis of Onshore Wind Energy Power Units during Earthquakes and Wind.* s.l., s.n., pp. 520--526.

Kjorlaug, R., 2013. *Seismic Response of Wind Turbines,* s.l.: s.n.

Kontoe, S., Zdravkovic, L., Potts, D. & E Salandy, N., 2007. *The use of absorbing boundaries in dynamic analyses of soil-structure interaction problems.* s.l., 12th international conference of international association for computer methods and advances in geomechanics.

Kourkoulis, R., Lekkakis, P., Gelagoti, F. & Kaynia, A., 2014. Suction caisson foundations for offshore wind turbines subjected to wave and earthquake loading: effect of soil–foundation interface. *Géotechnique,* Volume 64, pp. 171-185.

Kramer, S., Sideras, S. & Greenfield, M., 2016. The timing of liquefaction and its utility in liquefaction hazard evaluation. *Soil Dynamics and Earthquake Engineering,* Volume 91, pp. 133 - 146.

Leblanc, C. & Tarp-Johansen, N. J., 2010. *Monopiles in Sand. Stiffness and Damping,* s.l.: s.n.

McGann, C. R., Arduino, P. & Mackenzie-Helnwein, P., 2015. A stabilized single-point finite element formulation for three-dimensional dynamic analysis of saturated soils. *Computers and Geotechnics,* Volume 66, pp. 126-141.

Newman, J. N., 1977. *Marine hydrodynamics.* s.l.:MIT press.

Pecker A. & Pender MJ, 2000. *Earthquake Resistant Design of Foundations: NEW Construction.* Melbourne, s.n., pp. 313-332.

Pierson, J., Willard, J. & Moskowitz, L., 1964. A proposed spectral form for fully developed wind seas based on the similarity theory of S. A. Kitaigorodskii. *Journal of Geophysical Research,* Volume 69, pp. 5181-5190.

Pitilakis, K., 2010. *Geotechnical Earthquake Engineering.* Thessaloniki: ZHTH.

Risi, R. D., Bhattacharya, S. & Goda, K., 2018. Seismic performance assessment of monopile-supported offshore wind turbines using unscaled natural earthquake records. *Soil Dynamics and Earthquake Engineering,* Volume 109, pp. 154 - 172.

Roten, D., Fah, D. & Bonilla, L., 2014. Quantification of Cyclic Mobility Parameters in Liquefiable Soils from Inversion of Vertical Array Records. *Bulletin of the Seismological Society of America,* pp. 3115-3138.

Shadlou, M. & Bhattacharya, S., 2016. Dynamic stiffness of monopiles supporting offshore wind turbine generators. *Soil Dynamics and Earthquake Engineering,* Volume 88, pp. 15-32.

Sloan, S. W., 1987. Substepping schemes for the numerical integration of elastoplastic stress--strain relations. *International Journal for Numerical Methods in Engineering,* Volume 24, pp. 893-911.

Stockwell, R. G., Mansinha, L. & Lowe, R., 1996. Localization of the complex spectrum: the S transform. *IEEE transactions on signal processing,* Volume 44, pp. 998-1001.

Tehrani, F. S., Nguyen, P., Brinkgreve, R. B. & van Tol, A. F., 2016. Comparison of Press-Replace Method and Material Point Method for analysis of jacked piles. *Computers and Geotechnics,* Volume 78, pp. 38-53.

Tsuchiya, M., Ishihara, T. & Fukumoto, Y., 2006. The Wind Observation on the Pacific Ocean for Offshore Wind Farm.

Ushiyama, I., 2018. *Present Status and Target of Japanese Wind Power Generation.* s.l.:Springer International Publishing.

Watanabe, K., Pisanò, F. & Jeremić, B., 2017. Discretization effects in the finite element simulation of seismic waves in elastic and elastic-plastic media. *Engineering with Computers,* pp. 519-545.

Witcher, D., 2005. Seismic analysis of wind turbines in the time domain. *Wind Energy,* pp. 81-91.

Zahmatkesh, A. & Janalizadeh Choobbasti, A., 2017. Calibration of an advanced constitutive model for Babolsar sand accompanied by liquefaction analysis. *Journal of Earthquake Engineering,* Volume 21, pp. 679-699.

Zhang, Y. et al., 2017. Offshore wind farm in marine spatial planning and the stakeholders engagement: Opportunities and challenges for Taiwan. *Ocean \& Coastal Management,* Volume 149, pp. 69--80.

Zienkiewicz, O. C., Bicanic, N. & Shen, F. Q., 1989. Earthquake input definition and the trasmitting boundary in due tconditions. *Advances in computational nonlinear mechanics,* pp. 109-138.

Zienkiewicz, O. C. et al., 1999. *Computational geomechanics.* s.l.:Wiley Chichester.